

## BI-907828, a novel potent MDM2 inhibitor, inhibits glioblastoma brain tumor stem cells in vitro and prolongs survival in orthotopic xenograft mouse models

Xiaoguang Hao, Ravinder K. Bahia, Orsolya Cseh, Danielle A. Bozek, Sophia Blake, Jörg Rinnenthal, Ulrike Weyer-Czernilofsky, Dorothea Rudolph, and H. Artee Luchman

Arnie Charbonneau Cancer Institute, Hotchkiss Brain Institute, Cumming School of Medicine, University of Calgary, Calgary, Alberta, Canada (X.H., R.K.B., O.C., D.A.B., H.A.L.); Boehringer Ingelheim RCV GmbH & Co KG, Vienna, Austria (S.B., J.R., U.W.-C., D.R.)

**Corresponding Author:** H. Artee Luchman, PhD, Department of Cell Biology and Anatomy, Arnie Charbonneau Cancer Institute, Hotchkiss Brain Institute, Cumming School of Medicine, University of Calgary, 3330 Hospital Drive NW, Calgary, AB T2N 4N1, Canada ([aluchman@ucalgary.ca](mailto:aluchman@ucalgary.ca)).

### Abstract

**Background.** The tumor suppressor TP53 (p53) is frequently mutated, and its downstream effectors inactivated in many cancers, including glioblastoma (GBM). In tumors with wild-type status, p53 function is frequently attenuated by alternate mechanisms including amplification and overexpression of its key negative regulator, MDM2. We investigated the efficacy of the MDM2 inhibitor, BI-907828, in GBM patient-derived brain tumor stem cells (BTSCs) with different amplification statuses of MDM2, in vitro and in orthotopic xenograft models.

**Methods.** In vitro growth inhibition and on-target efficacy of BI-907828 were assessed by cell viability, co-immunoprecipitation assays, and western blotting. In vivo efficacy of BI-907828 treatments was assessed with qPCR, immunohistochemistry, and in intracranial xenograft models.

**Results.** BI-907828 decreases viability and induces cell death at picomolar concentrations in both MDM2 amplified and normal copy number *TP53* wild-type BTSC lines. Restoration of p53 activity, including robust p21 expression and apoptosis induction, was observed in *TP53* wild-type but not in *TP53* mutant BTSCs. shRNA-mediated knock-down of *TP53* in wild-type BTSCs abrogated the effect of BI-907828, confirming the specificity of the inhibitor. Pharmacokinetic-pharmacodynamic studies in orthotopic tumor-bearing severe combined immunodeficiency (SCID) mice demonstrated that a single 50 mg/kg p.o. dose of BI-907828 resulted in strong activation of p53 target genes p21 and MIC1. Long-term weekly or bi-weekly treatment with BI-907828 in orthotopic BTSC xenograft models was well-tolerated and improved survival both as a single-agent and in combination with temozolomide, with dose-dependent efficacy observed in the MDM2 amplified model.

**Conclusions.** BI-907828 provides a promising new therapeutic option for patients with *TP53* wild-type primary brain tumors.

### Key Points

- BI-907828 decreases viability and induces cell death in *TP53* wild-type GBM BTSC lines.
- BI-907828 dramatically improves survival in orthotopic GBM xenograft models.
- BI-907828 is a promising new therapeutic option for *TP53* wild-type GBM patients.

## Importance of the Study

MDM2 inhibitors block the interaction between p53 and its key negative regulator, MDM2, and represent a new therapeutic concept for cancer. MDM2 inhibitors are designed to restore p53 activity in *TP53* wild-type tumors and several MDM2 inhibitors are currently being evaluated for clinical development. BI-907828 is a novel, potent oral MDM2 inhibitor suitable for intermittent dose schedules with optimized drug-like properties such as high permeability, good physiological solubility, a low

systemic clearance, and high oral bioavailability. Here, we show that BI-907828 crosses the blood-brain barrier and that treatment of *TP53* wild-type patient-derived GBM models, with or without MDM2 amplification, induces tumor cell death, reduces tumor burden, and increases survival using weekly dose schedules over an extended period. BI-907828 provides a promising novel therapeutic option for patients with *TP53* wild-type primary brain tumors.

The tumor protein 53 (TP53/p53), the so-called “guardian of the genome,” is a pivotal tumor suppressor protein and a mainstay of the body’s cellular anti-cancer defense system.<sup>1</sup> As a transcription factor, p53 regulates multiple downstream target genes that are involved in cell cycle arrest or senescence, DNA repair, and apoptosis.<sup>1–4</sup> Under normal conditions it is therefore critical that intracellular levels of p53 are kept at a low, basal state, which is achieved by rapid (proteasome-mediated) degradation of p53.<sup>1–5</sup> In cells that are exposed to stress signals or are damaged, TP53 is rapidly activated while it is kept in check in normal cells and in tumor cells in which the *TP53* gene is frequently mutated. Although the incidence of *TP53* mutations differs significantly between different cancer types, *TP53* is one of the most frequently mutated genes in human cancers with about 50% of all cancers displaying mutations or deletions in this gene.<sup>6,7</sup> Remaining human cancers have tumors with *TP53* wild-type status but the function of p53 is frequently attenuated by other mechanisms, including overexpression or amplification of its key negative regulator, human MDM2.<sup>6,7</sup>

Glioblastoma (GBM) is the most common and aggressive form of brain cancer and despite the current therapy of surgical resection, followed by radiation and chemotherapy, the median survival of patients is a mere 15 months.<sup>8</sup> GBM is an invasive, highly drug-resistant, and ultimately incurable disease that requires continued research into its inherent biology to identify novel therapeutic avenues. In glioma, *TP53* mutations are frequent in grade II and III astrocytomas and consequently in secondary GBMs that arise from the progression of these lower-grade tumors.<sup>9</sup> The Cancer Genome Atlas (TCGA) findings have demonstrated that direct mutation or homozygous deletion of *TP53* occurs in 35% of primary GBMs, particularly in association with *IDH1/2* mutations.<sup>10,11</sup> Moreover, nearly half of all GBMs have functional inactivation of p53 due to deletion or amplification of *MDM2* or *MDM4* or *CDKN2A*<sup>10</sup> resulting in accelerated p53 degradation and inactivation of p14ARF inhibition of MDM2 function. Thus, while MDM2 inhibitors are not of relevance in tumors with TP53 mutations, tumors with *CDKN2A* deletion or MDM2 amplification, and those retaining a wild-type *TP53* status, are potentially treatable with MDM2 inhibitors (reviewed in Ref. 12).

Preclinical data show that mutations in *TP53* not only contribute to tumor development but also maintain

tumor growth of established tumors, as restoration of p53 function by genetic means in established *TP53* mutant tumors causes tumor regressions in preclinical cancer models.<sup>13–16</sup> Based on these data, stabilization and activation of wild-type p53 by the inhibition of p53 binding to its negative regulator MDM2 have been explored as a novel approach to cancer therapy. Several MDM2-p53 protein-protein interaction (PPI) inhibitors are currently being evaluated in early clinical development<sup>16–19</sup> (reviewed in Ref. 20). Idasanutlin (RG7388), has shown promising results in a phase I trial in patients with acute myeloid leukemia (AML) and has advanced to phase III trial for relapsed/refractory AML.<sup>21</sup> AMG-232 is in phase I clinical trials for GBM, sarcoma, and myeloid malignancies.<sup>22</sup> However, the development of resistance to MDM2 inhibitors, based on mutations in *TP53*, has been reported.<sup>23</sup> Additionally, thrombocytopenia has been further shown to be an ongoing concern in this class of inhibitors.<sup>17,23–26</sup> Hence there is a need for less frequently dosed MDM2 inhibitors to potentially improve the therapeutic window for these inhibitors.

BI-907828 is a MDM2 inhibitor that blocks the interaction between MDM2 and p53 by binding to MDM2.<sup>27–32</sup> This prevents MDM2 from inactivating p53, thereby restoring p53 function in tumors with wild-type p53 and inducing target gene expression involved in processes such as cell-cycle arrest and DNA repair, senescence, and apoptosis.<sup>32</sup> BI-907828 is undergoing investigation in several phase I trials as a monotherapy in patients with *TP53* wild-type solid tumors.<sup>33,34</sup>

We investigated the efficacy of BI-907828 in *TP53* wild-type GBM patient-derived brain tumor stem cell (BTSC) lines with different amplification statuses of MDM2 both in vitro and in orthotopic xenograft models. We find that BI-907828 decreases viability and induces cell death in both MDM2 amplified and normal copy number (CN) *TP53* wild-type GBM BTSC lines and demonstrates in vivo on-target efficacy in orthotopic models derived from these cell lines. Long-term treatment with BI-907828 as a monotherapy or in combination with the standard of care temozolomide (TMZ) is well-tolerated and a significant survival benefit was observed in all treatment groups compared to vehicle-treated control animals. BI-907828 should be further evaluated as a promising novel therapeutic option for patients with *TP53* wild-type primary brain tumors.

## Materials and Methods

### Cell Culture

GBM BTSC lines ( $n = 19$ ) were cultured from a series of tumor specimens obtained during surgical resection and approval from the University of Calgary Ethics Review Board as previously described<sup>35–39</sup> and in [Supplemental Methods](#). Human induced pluripotent stem cells (hiPSCs) were obtained from American Type Culture Collection (ATCC). Neural progenitors (NPs) were cultured from hiPSCs as per ATCC protocols and astrocytes derived from HF-NSCs (human fetal neural stem cells) and hiPSCs-NSCs were cultured in the Dulbecco's Modified Eagle Medium with 10% fetal bovine serum.

### MDM2 CN and TP53 Status

MDM2 status was determined from previous exome sequenced (30x coverage) data for the BTSC lines used in this study. The algorithm used to determine CN status was an Hidden Markov model (HMM)-based approach as described.<sup>40</sup> The CN values mean the CN status compared to normal and have integer values from 0 to 5: 0–2–copy loss; 1–one–copy loss; 2–no copy change; 3–one–copy gain; 4–2–copy gain; 5–3 or more copies gain. *TP53* somatic mutations were detected by variant calling from SAMTools and Strelka.

### Viability and Cytotoxicity Assays

Four GBM-derived BTSC lines with an MDM2 CN amplification of  $CN \geq 3$ , 7 BTSC lines with MDM2 CN 2 on a *TP53* wild-type background and 8 BTSC lines with *TP53* mutant background ([Supplemental Table 1](#)), NPs, HF Astros, and ips Astros were tested in concentration-response experiments with BI-907828. One thousand to two thousand five hundred cells/well were plated in 96-well plates. Increasing drug concentrations were added to cells after 24 h with 3 replicate wells per concentration. Viability was assessed for cell lines between 5 and 14 days by generating  $IC_{50}$  dose-response curves using alamarBlue™ assays. IncuCyte™ Cytotox Red Reagent (Sartorius) was used to measure cell death following treatment with BI-907828. Cells were allowed to form neurospheres for 3–5 days and treated for 48 h with different concentrations of BI-907828. Cytotox Red was added, and cells were imaged for 8 h. Percent death was calculated as the percent red fluorescence over the percent total cell occupancy. Details of drugs and stock concentrations are provided in [Supplemental Methods](#).

### Annexin V Cell Survival Assays

The cell viability in BI treated and untreated p53 knock-down BTSC lines were assessed with the Alexa Fluor™ 488 Annexin V Apoptosis Detection Kit as per manufacturer's guidelines (BD Biosciences). Briefly, the BTSC cells were dissociated and  $1.0 \times 10^5$  cells were resuspended in binding

buffer and stained with Annexin V- Alexa Fluor™ 488 and 7-amino actinomycin D (7AAD) for 15 min. Flow cytometry analysis was performed using CytoFLEX LX (Beckman Coulter) and results were analyzed using FACSDiva software version 6.1.3 (BD Biosciences).

### In Vivo Experiments

All animal procedures were performed according to our animal ethics protocol (AC21-0162), approved by the Animal Care Committee of the University of Calgary and operating under the Guidelines of the Canadian Council on Animal Care. A total of 100 000 viable BTSCs were resuspended in 2  $\mu$ l of phosphate buffered saline for stereotactic implantation into the striatum of the right cerebral hemisphere of 6- to 8-week-old CB-17 SCID mice (Charles River) as previously described<sup>36</sup> and in [Supplemental Methods](#). For pharmacokinetic/pharmacodynamic (PK/PD) studies, on day 64 post-tumor implantation (BT48 model) and day 60 post-tumor implantation (BT67 model), 3 mice from each cell line were used as a pretreatment group and the remaining mice were treated with a single oral dose of 50 mg/kg BI-907828 and randomized for collection of samples at various time points (6 h, 24 h, 48 h, 72 h, and 168 h post-dose). Plasma, brain, and thigh/leg muscle samples were collected from  $n = 3$  mice per time point. For Kaplan–Meier studies, treatment conditions were vehicle controls, 2 mg/kg, 10 mg/kg, 15 mg/kg BI-907828, 50 mg/kg BI-907828, 30 mg/kg TMZ, and combination treatments of 30 mg/kg TMZ + 15 mg/kg BI-907828 or 30 mg/kg TMZ + 2 mg/kg BI-907828 (BT89 study). Treatments were started on day 43, day 58, and day 50 post-implantation with BT48, BT67, and BT89 respectively. Treatments were qw with 2 mg/kg, 10 mg/kg, 15 mg/kg BI-907828, or 30mg/kg TMZ and combination arms and q2w treatment for the 50 mg/kg BI-907828 arm in the BT48 and BT 67 models, continued for the duration of the study. Animals were sacrificed when experimental endpoints, according to animal care guidelines, were reached. Brains from each group were cryo-sectioned and stained with H&E and anti-human nucleolin antibody (1:1000, Abcam, # AB13541, Cambridge, UK) and Ki67 (1:250, Vector labs, VP-K451).

### mRNA Expression

Following RNA isolation and cDNA synthesis ([Supplemental methods](#)), mRNA expression of human and mouse genes was analyzed with the following primers from Life Technologies: CDKN1a (p21) (cat # Hs99999142\_m1, Human only), GAPDH (cat# Hs99999905\_m1, Human only), (CDKN1a (p21) Mm01303209\_m1, Mouse only), GAPDH (cat# Mm99999915\_g1, Mouse only), GDF15/MIC-1 (cat# Hs00171131\_m1, Human only). qPCR was performed using the MxPro3005P under the following conditions: Initial denaturation, 95°C 1 cycle for 10 min, annealing 15 s at 95°C, 40 cycles and extension at 60°C for 1 min. Ct values were normalized to GAPDH of the respective species, generating delta Ct values: Ct value for gene of interest – Ct value for GAPDH = delta CT value. Relative expression values were determined based on the following formula:  $2^{-\Delta\Delta Ct}$  values. Fold changes of the gene of interest were calculated based

on the following formula:  $2^{-\Delta\text{DCt}}$  treatment group/ $2^{-\Delta\text{DCt}}$  control group.

### Western Blotting

Total protein samples were extracted using radioimmunoprecipitation assay (RIPA) buffer and used for western blotting. Blots were probed with target and control antibodies overnight at 4°C, followed by washing and incubation with horseradish peroxidase-conjugated secondary antibodies. Blots were imaged with SuperSignal and Amersham Imager 600 (General Electric). A full list of antibodies used is provided in [Supplemental Methods](#).

### Co-immunoprecipitation Assays

BTSC lines, BT48, BT67, and BT119 were treated with 10 nM BI-907828 or dimethyl sulfoxide (DMSO) for 24 h. Immunoprecipitation reactions (IP) were performed as described in [Supplemental Methods](#).

### Proximity Ligation Assays

In situ proximity ligation assays (PLAs) were performed to detect PPIs between the proteins of interest using (PLA) Duolink® Kit (cat# DUO92002, Sigma-Aldrich) as per manufacturer's protocol and [Supplemental Methods](#). Slides were imaged on a high-capacity Olympus VS120 slide scanner at 40× magnification. A minimum of 30 nuclei were processed for PLA foci quantification using the Fiji Image analysis tool with consistent noise level settings for all images.

### Stable Lentiviral Knockdown

Stable knockdown of TP53 or MDM2 were performed using three independent shRNA sequences for each gene ([Supplemental Methods](#)) and their respective scrambled shRNA controls (GeneCopoeia). The lentiviral particles were generated as previously described.<sup>41</sup> The shRNA sequences for targeting TP53 and MDM2 were tagged with red-fluorescent proteins (mCherry) or green- (GFP) respectively as a marker of transduction efficiency. TP53 knockdown cells were selected using hygromycin and puromycin was used for the selection of MDM2 knockdown cells. Knockdown efficiency of each shRNA sequence was validated by western blot.

### Statistical Analyses

Images of BTSC cultures were captured using the IncuCyte Zoom (Essen Bioscience). An Olympus Slide Scanner was used to image the brain sections. OlyVIA (Olympus Life Science) software was used to analyze the images. Nonlinear curve fit/log inhibitor vs normalized response formula was used to generate  $IC_{50}$  data. Data illustrated in bar graphs show mean  $\pm$  SD and statistically significant differences were evaluated by means of analysis of variance (ANOVA). Statistical differences in median survival were determined by the log-rank test for Kaplan Meier studies.

Analyses were performed using GraphPad Prism Version 9.0.

## Results

### BI-907828 Decreases BTSC Viability at Picomolar Concentrations

We first confirmed *MDM2* CN, *TP53* mutational, and *MGMT* promoter methylation status of the (previously whole genome sequenced<sup>42</sup>) BTSC lines used in this study ([Supplemental Table 1](#)). We further verified the protein expression of MDM2 and p53 for the 19 BTSC lines used in this study by western blotting ([Figure 1A](#)). We then asked whether BI-907828 could reduce BTSC viability. Four *TP53* wild-type BTSC lines with an *MDM2* CN of  $\geq 3$ , 7 *TP53* wild-type BTSC lines with a *MDM2* CN of 2 and 8 *TP53* mutant cell lines with a *MDM2* CN of 2 were treated with BI-907828 at increasing concentrations between 0.5 pM and 40 nM in serum-free culture conditions. We also used NP cells and astrocytes derived from iPSCs (iPS Astros) and astrocytes derived from normal neural fetal cells (HF Astros) as additional controls. BI-907828 was potent at decreasing viability in both *MDM2* amplified and normal CN *TP53* wild-type cell lines ([Figure 1B](#) and [D](#) and *MDM2* status in [Supplemental Table 1](#)). BI-907828 decreased the viability of the NPs, iPS Astros, and HF Astros but at much higher  $IC_{50}$  (1–2 log fold) values than for the BTSC cells. The  $IC_{50}$  values for the 11 *TP53* wild-type BTSC cultures tested ranged from 21.1 pM to 424.9 pM ([Figure 1C](#)).  $IC_{50}$  values were not derivable for the mutant cell lines ([Figure 1D](#)).

TMZ is currently the standard of care chemotherapy for GBM and is widely used for most GBM patients. We thus tested a clinically relevant concentration of TMZ (10  $\mu\text{g}/\text{ml}$ )<sup>43</sup> in 8 BTSC ([Supplemental Figure 1](#)) lines to verify sensitivity to TMZ based on *MGMT* promoter methylation status. TMZ response was as predicted by *MGMT* methylation status, with methylated cell lines BT48, 50, 67, and 127 responding to TMZ treatment and unmethylated cell lines BT69, 140 and 208, and 301 being less sensitive to TMZ treatment ([Supplemental Figure 1](#)).

BI-907828 appears to be highly effective at decreasing the viability of *TP53* wild-type BTSCs in vitro, irrespective of *MDM2* CN or *MGMT* promoter methylation status ([Supplemental Table 1](#)).

### BI-907828 Inhibits Proliferation and Induces Cell Death in TP53 Wild-type But Not TP53 Mutant BTSCs

Our response data showed reduced cell viability at low concentrations of BI-907828 in *TP53* wild-type BTSCs, suggesting that MDM2 may be a suitable target for pharmacological modulation in glioma with wild-type *TP53* status. We treated a mutant (BT73) line alongside *TP53* wild-type lines (BT48 and BT67) and assessed cell viability after 5 days by Alamar blue staining. We observed that while both *TP53* wild-type cell lines showed a strong reduction in growth when treated with the lowest concentration of 12.8 pM and a complete abrogation of cell viability at higher



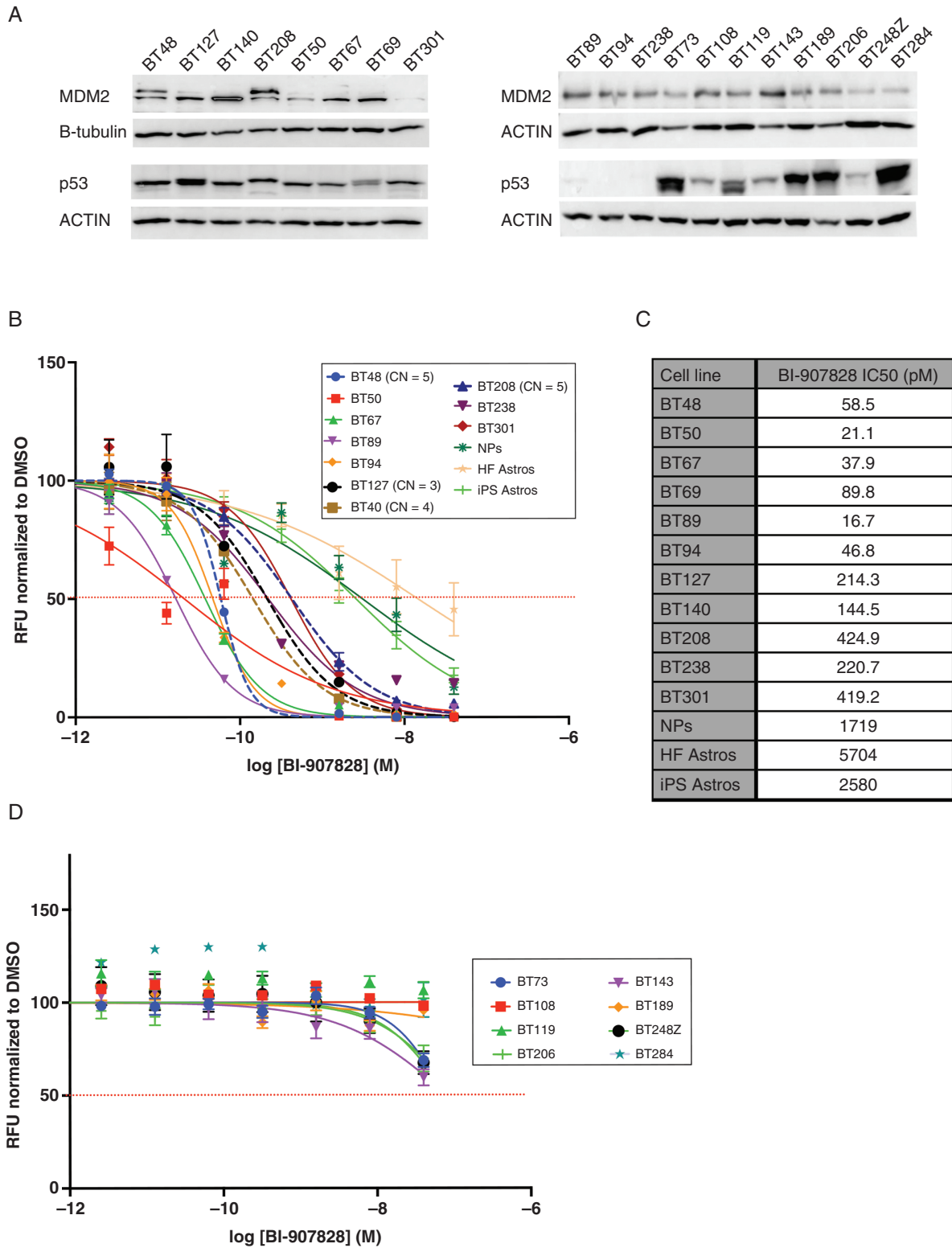


**Figure 1.** Effects of BI-907828 on viability of *TP53* wild-type GBM brain tumor stem cell (BTSC) lines with amplified or normal copy numbers (CNs) of *MDM2*. (A) Protein expression of *MDM2* and *p53* in BTSC lines. (B) BI-907828 decreased cell viability in *TP53* wild-type BTSCs with *MDM2* amplified or normal CN status. (C) IC<sub>50</sub> values extracted from IC<sub>50</sub> curves are depicted in (B).

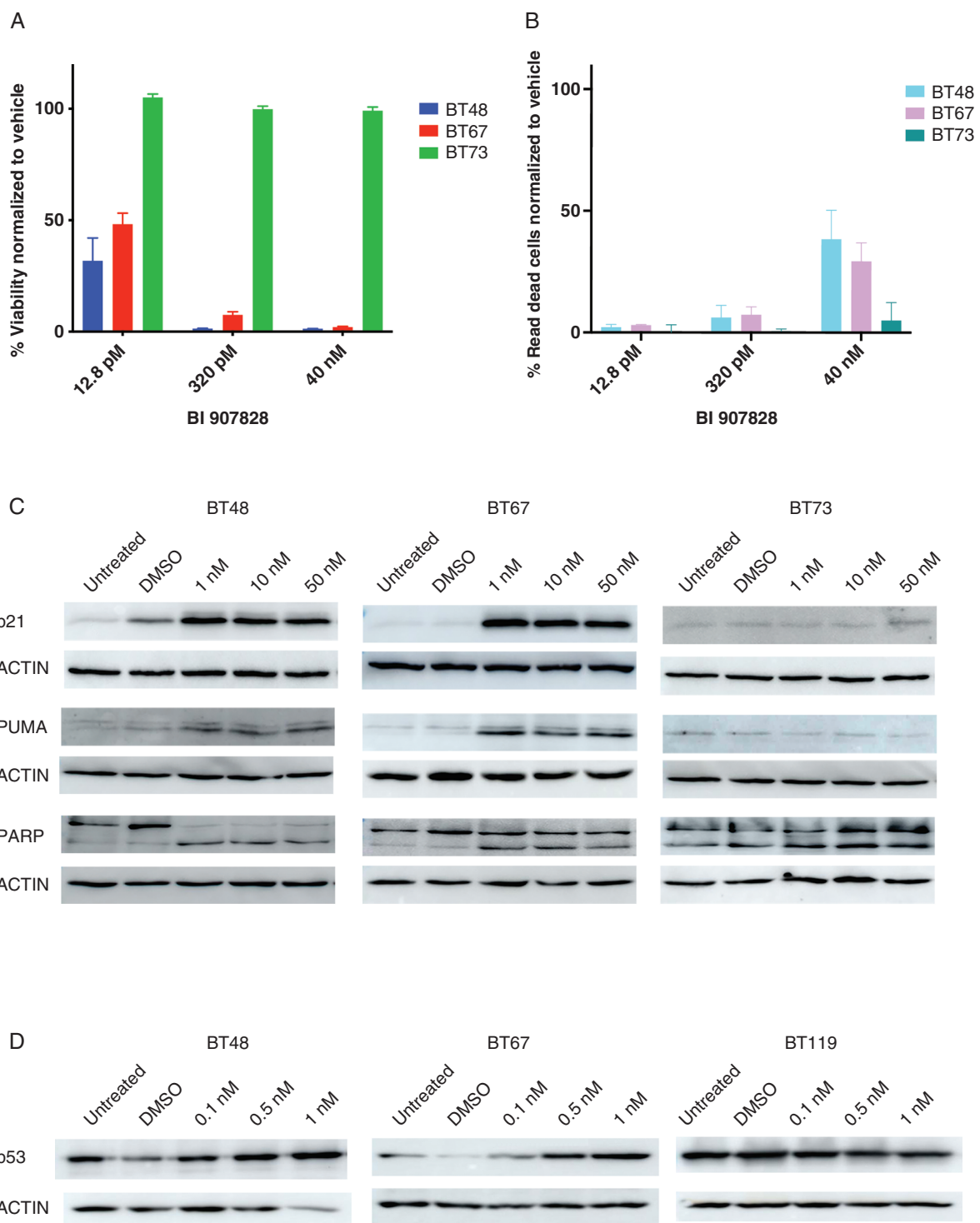


**Figure 2.** BI-907828 effectively decreases viability, increases cell death and has on-target activity on downstream targets in *TP53* wild-type brain tumor stem cells (BTSCs). (A) Relative viability and (B) relative cell death in *TP53* wild-type cell lines with either MDM2 amplified (BT48) or normal MDM2 copy number (CN) (BT67) and *TP53* mutant normal MDM2 CN (BT73). (C) p21 and PUMA protein expression levels and cleaved poly-ADP ribose polymerase (PARP) following treatment with 12.8 pM, 320 pM, and 40 nM of BI-907828 in *TP53* wild-type BT48 and BT67 cell lines and *TP53* mutant cell-line BT73. Actin was used as a loading control. Shown as representative blots of 3 biological replicates. Error bars represent the standard error of the mean for  $n=3$  biological replicates.  $P$ -values were calculated using one-way ANOVA with Tukey's multiple comparisons tests (A, B), \* $P < .01$ , \*\* $P < .001$ , \*\*\*\* $P < .0001$ . n.s. = not significant.

concentrations (Figure 2A, Supplemental Figure 2), TP53-mutant BT73 showed no response even at the highest concentration of 40 nM (Figure 2A, Supplemental Figure 2). Using a cell-impermeable fluorescent DNA stain, we further found that treatment increased cell death after 48 h treatments in the 2 TP53 wild-type BTSC lines with cell death observed in TP53 mutant BT73 BTSC line only at the highest concentration tested (Figure 2B, Supplemental Figure 2B).

We further confirmed that BI-907828 induced upregulation of p53 transcriptional targets p21 and PUMA (Figure 2C), mediating p53-dependent cytostasis and apoptosis, respectively, in TP53 wild-type BT48 and BT67, but not in the TP53 mutant BT73 cell line. We observed increased cleaved PARP, in the TP53 wild-type BTSC lines with increasing concentrations of BI-907828 (Figure 2C), further demonstrating cell death and apoptosis induction in the TP53 wild-type lines following BI-907828 treatments. In contrast, the fast-growing TP53 mutant BT73 cell line, which displays higher basal levels of cell death in neurosphere cultures, showed no noticeable increase in the levels of cleaved PARP (Figure 2C) or uptake of the cell-impermeable fluorescent DNA stain (Supplemental Figure 2B) at even the highest concentrations of BI-907828 versus DMSO control.

We further showed an increase of the protein level of p53 in the TP53 wild-type cell lines BT48 and BT67 following treatment (24 h) with low doses of BI-907828 (Figure 2D) as well as an increase in total ubiquitinated proteins in these 2 cell lines (Supplemental Figure 2C). These effects were not observed in a TP53 mutant cell line, BT119 (Figure 2D and Supplemental Figure 2C). Taken together, these data show that BI-907828 inhibits the interaction of MDM2 with p53 and the resulting degradation of wild-type p53. This may then engage the proteasome degradation machinery and accumulation of ubiquitinated proteins ultimately leading to increased cell death.

Taken together, these data confirm that BI-907828 is effective at reducing viability and inducing apoptosis in TP53 wild-type BTSCs in vitro.

### BI-907828 Disrupts the Specific Interaction Between MDM2 and p53 in p53 Wild-type BTSCs

We next asked whether the inhibitory effects of BI-907828 were specific to the interaction between MDM2 and p53. We performed co-immunoprecipitation assays, following treatment of BTSCs with 10 nM BI-907828 or DMSO vehicle control in 2 TP53 wild-type cell lines (BT48 and BT67) and a TP53 mutant (BT119) cell line. We observed a reduction in the level of immunoprecipitated p53 protein, when an MDM2 antibody was used for IP in BI-907828-treated BTSC lysates compared to vehicle-treated samples in the p53 wild-type cell lines but not in the mutant cell line (Figure 3A(i)). Conversely, a reduced pull down of MDM2 protein was observed following IP with a p53 antibody, in BI-907828 treated BTSC lysates compared to vehicle-treated samples (Figure 3A(ii)). Treatment with BI-907828 did not disrupt the interaction between MDM2 and MDM4 (Figure 3A(iii)).

We further confirmed these findings using in situ PLAs. We observed a significantly higher number of PLA foci per

nuclei, following incubation with anti-p53 + anti-MDM2 antibodies, in vehicle-treated cells compared to BI-907828 treated TP53 wild-type cells (Figure 3B(i, ii)). As expected, there were fewer foci in the BT119 TP53 mutant cell line and no difference was observed in vehicle or BI-907828 treatments (Figure 3B(i, ii)). Furthermore, there was no effect of the inhibitor on the PLA foci in samples probed with anti-MDM2 + anti-MDM4 antibodies (Figure 3B(i, ii)). These data further confirm that BI-907828 specifically disrupts the interaction between MDM2 and p53.

### TP53 Knock-down Abrogates the Effect of BI-907828 in p53 Wild-type Cells

We next asked whether the p53 knockdown would reduce the effect of BI-907828. We used 3 different shRNA sequences to knock-down TP53 in the TP53 wild-type cell lines BT48 and BT67 and in the TP53 mutant cell line, BT119 (Figure 4A). We observed a decrease in sphere size in scrambled shRNA targeted control cells treated with BI-907828, but no effect of BI-907828 on the TP53-knock down cells in the TP53 wild-type cell line BT48, following TP53 knockdown (Figure 4B). We further confirmed these results in BTSC lines treated with 10 nM BI-907828 for 5 days. Annexin V/7AAD staining followed by flow cytometric analysis showed a greater increase in the frequency of Annexin V+/7AAD+ cells (dead cells) in scrambled shRNA targeted p53 wild-type cell lines (BT48 and BT67) than in the knockdown cells treated with BI-907828 (Figure 4C, Supplemental Figure 3A). These results are analogous to the lack of effect observed when treating the p53 mutant cell line BT119 with BI-907828 (Figure 4C, Supplemental Figure 3A).

We further investigated the effect of knocking down MDM2 in p53 wild-type BTSCs. (Supplemental Figure 3B and C). While the shRNA target sequences reduced the protein expression of MDM2 in the p53 wild-type cell lines, we observed increased cell death in the targeted cell lines following selection as evidenced by smaller neurosphere sizes (Supplementary Figure 3C). We were not able to distinguish drug effects of the BI-907828 inhibitor from the intrinsic cell death observed with the knock-down of MDM2 in these cell lines. We have previously reported MDM2 as being a highly essential gene for viability in GBM BTSC lines.<sup>41</sup> These data further support that targeting MDM2 in TP53 wild-type GBM cells is a promising strategy in GBM.

### Administration of a Single Dose of BI-907828 Demonstrates Target Gene Induction in Intracranial Orthotopic Xenografts of BTSCs

Previous pharmacokinetic studies with BI-907828 showed low systemic clearance and high bioavailability in mice, rats, dogs, and minipigs.<sup>27</sup> Here, we assessed brain concentration (PK) and PD biomarker modulation of BI-907828 in 2 orthotopic GBM patient-derived BTSC models (BT48 and BT67) in SCID mice. Tumor engraftment was confirmed in sentinel animals on day 44 (BT48 model) or day 41 (BT67 model) (Figure 5A). On day 64 post-tumor implantation (BT48 model) or on day 60

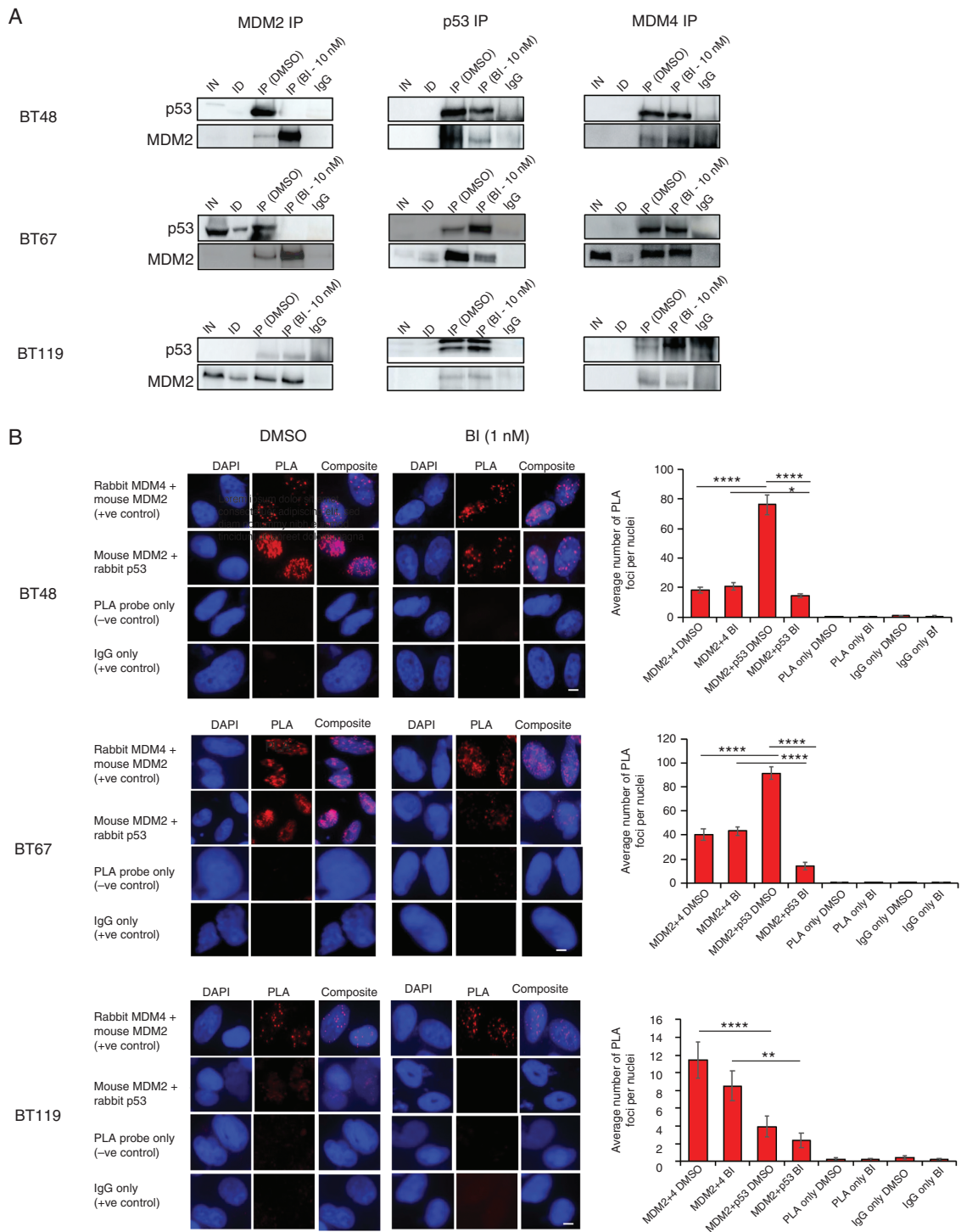


**Figure 3.** BI-907828 disrupts the interaction between MDM2 and wild-type p53 in brain tumor stem cells (BTSCs). (A) Co-immunoprecipitation assays in dithiobis succinimidyl propionate (DSP) crosslinked BT48, BT67, and BT119 cells. IP-immunoprecipitation, ID-immunodepleted samples, immunoglobulin G (IgG)-antibody controls for nonspecific pull-down. (B) (i) In situ proximity ligation assays (PLAs) determined a disruption of protein-protein interactions between MDM2 and p53 following treatment with 1 nM BI-907828 in p53 wild-type, BT48 and BT67 cells but not in p53 mutant, BT119 cells. (ii) Quantitative representation of the average number of PLA foci counted in 30 nuclei/reaction in BI-907828 treated BT48, BT67, and BT119 cells. Data are represented as mean  $\pm$  SE;  $N = 3$ . \*\*\*\* $P < .000$ . MDM2/4 protein-protein interaction was used as positive control and PLA probe only and IgG only as negative controls for the assay. Scale bar: 10  $\mu$ m.



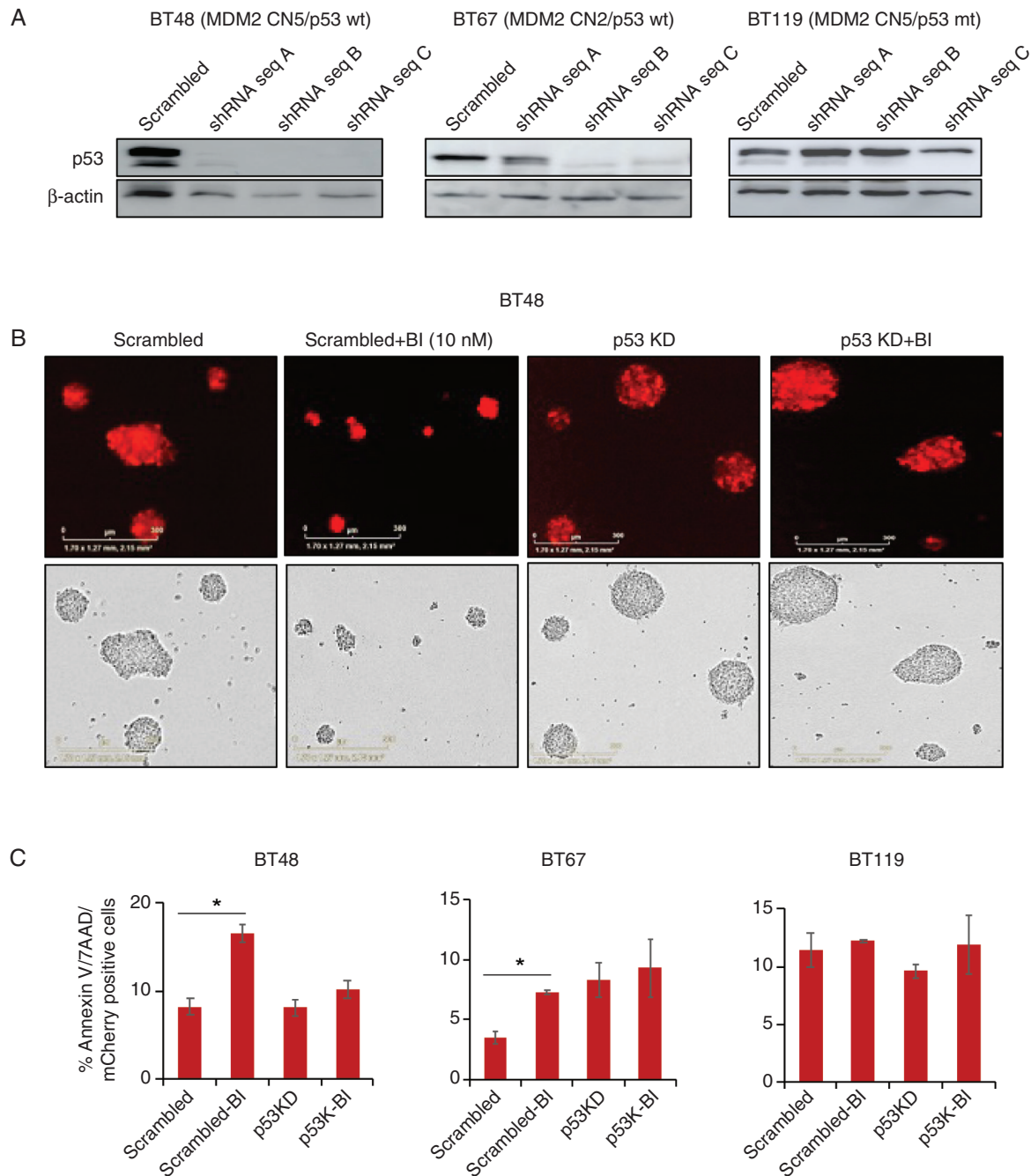


**Figure 4.** The effect of BI-907828 is abrogated in p53 knock-down brain tumor stem cells (BTSCs). (A) Validation of p53 knockdown by Western blot using 3 independent shRNAs to target p53 in wild-type BT48, BT67, and mutant BT119 cells. (B) Fluorescent and brightfield images of shRNA mediated KD of p53 in BT48 cells and their respective scrambled control images. Treatment with BI-907828 showed a decrease in sphere size in scrambled control BT48 but not in p53 KD cells. Scale bar: 300  $\mu$ m. (C) Annexin V cell survival assays in BT48, BT67, and BT119 p53 KD and in their respective scrambled control cells with and without BI-907828 treatment. (Unpaired *t*-test, \**P* < .05; data are represented as mean  $\pm$  SE; *N* = 3).

post-tumor implantation (BT67 model), SCID mice with established brain tumors were treated with a single oral dose of 50 mg/kg BI-907828 and plasma, brain, and thigh/leg muscle samples were collected from *n* = 3 mice per time point at various time points post-dose (pretreatment, 6 h, 24 h, 48 h, 72 h, and 168 h post-dose). Plasma

concentration, brain tissue concentration, muscle tissue concentration, and PD biomarker modulation (= p53 target gene induction, ie, induction of mouse CDKN1a [p21] mRNA, human CDKN1a [p21] mRNA, or human GDF15 [MIC-1] mRNA = human MIC-1 mRNA) in brain tissue was assessed in these samples. The non-engrafted

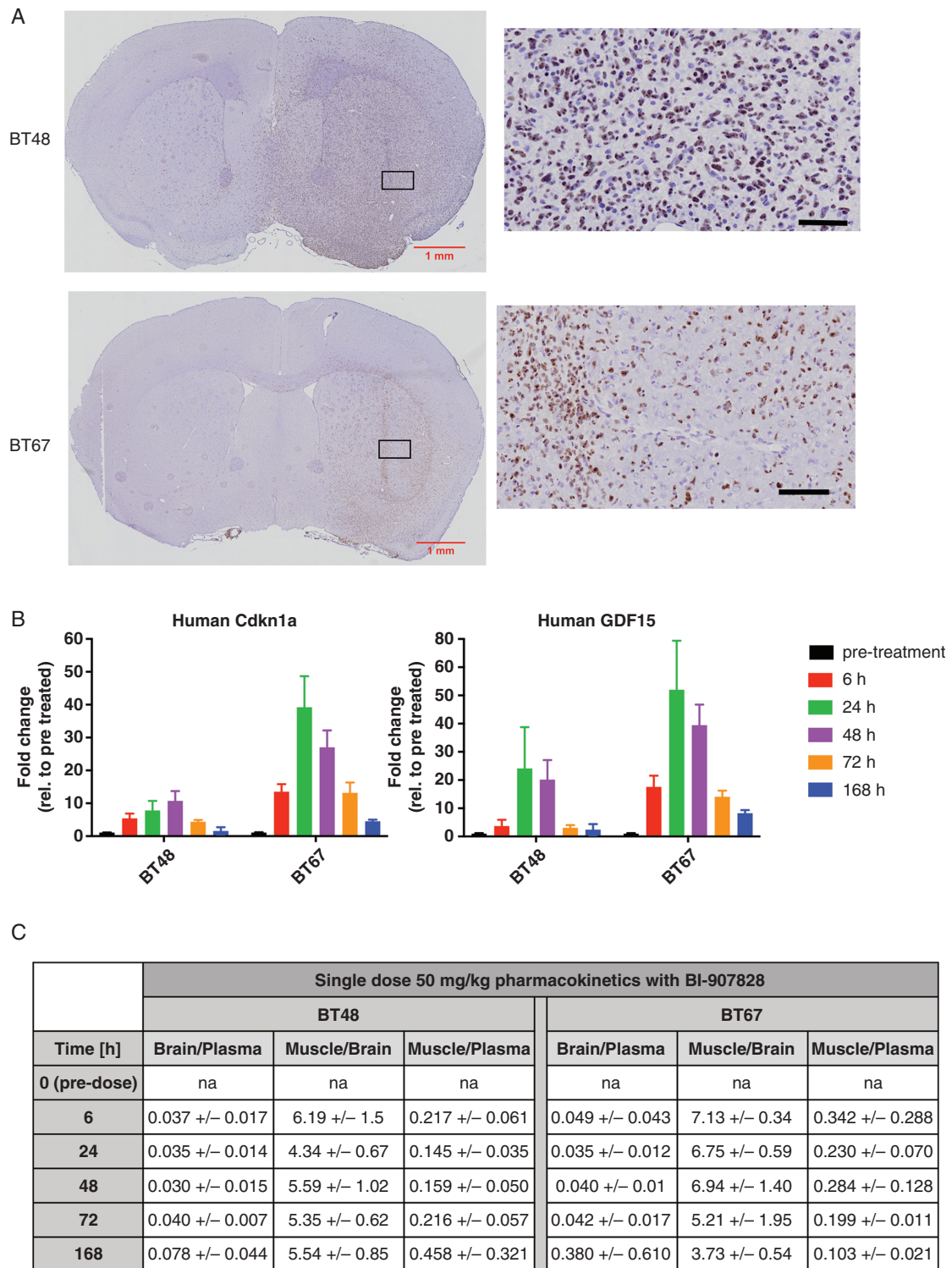


**Figure 5.** Treatment of GBM patient-derived brain tumor stem cells (BTSCs) tumor-bearing mice with a single dose of BI-907828 leads to a significant increase in PD biomarkers in the brain. (A) Anti-human nucleolin immunohistochemistry (IHC) on tumor sections from satellite animals on day 44 for the BT48 model and on day 41 for the BT67. (B) Treatment with a single oral dose of BI-907828 at 50 mg/kg led to a significant increase in all measured human indirect target engagement PD biomarkers. PD biomarkers tested (CDKN1a and GDF15 shown) in both models (BT48 and BT67), as assessed by their mRNA induction. Human CDKN1a mRNA induction normalized to human GAPDH mRNA (fold change relative to pretreatment levels). Human GDF15 (MIC-1) mRNA induction normalized to human GAPDH mRNA (fold change relative to pretreatment levels). (C) Mean brain/plasma, muscle/brain, and muscle/plasma ratios of BI-907828 in BT48 and BT67 tumor-bearing mice after a single dose of 50 mg/kg. Mean values and standard deviations are derived from measurements of 3 individual animals for each time point. Scale bars on left panels represent 1 mM and scale bars on right higher magnification panels represent are 100  $\mu$ m.

brain hemisphere was assessed for tissue concentration of BI-907828, and the engrafted hemisphere was used to assess PD biomarker modulation. Strong PD biomarker induction was observed for all human indirect target engagement PD biomarkers tested (CDKN1a [p21] and GDF 15 [MIC-1]), in a time-dependent manner in both models (BT48 and BT67), as assessed by their mRNA induction (Figure 5B). No induction was observed for mouse CDKN1a (Supplemental Figure 5A). These data show that target gene induction was detected in the human tumor lesion but not in the surrounding mouse brain tissue.

Treatment of tumor-bearing mice with a single oral dose of BI-907828 at 50 mg/kg led to high plasma concentrations with a mean  $c_{max}$  of 13.5  $\mu$ M in the BT48 tumor model, reached at 6 h, and 12.0  $\mu$ M in the BT67 model, reached at 24 h (Supplemental Figure 5B). Plasma concentrations remained high ( $> 2 \mu$ M) from 6 to 72 h in both models and dropped to concentration levels below 1  $\mu$ M at 168 h (Supplemental Figure 5B). Overall, variability in plasma concentrations between individual animals was high in both studies (Supplemental Figure 5B). However, average brain and muscle concentrations from 3 mice showed a high correlation (Figure 5C). Therefore, brain/plasma, muscle/plasma, and muscle/brain ratios could be determined with high accuracy. At time points between 6 and 72 h, brain/plasma ratios were determined to be  $0.038 \pm 0.011$  and muscle/plasma ratios were determined to be  $0.22 \pm 0.09$ . Muscle/brain ratios were determined to be constant with  $5.67 \pm 1.1$  on average over all animals tested.

Taken together, these PK-PD studies thus demonstrate that a single oral dose of BI-907828 leads to exposure levels that are sufficient to modulate p53 target genes in brain tumor tissue in 2 BTSC-derived orthotopic GBM models. These findings suggest that BI-907828 can pass the blood-brain barrier and confirm previous findings of low systemic clearance.

### Treatment With BI-907828 Increased Median Overall Survival in Intracranial Orthotopic Xenograft BTSC Models

We next assessed the efficacy of BI-907828 treatment in vivo with orthotopic xenografts of both a *MDM2* amplified (BT48; CN = 5) and a normal CN (BT67; CN = 2), TP53 wild-type BTSC model. BI-907828 was administered orally once a week at 15 mg/kg. For the 50 mg/kg treatment arm, treatment was started at 51 days and 58 days post-tumor cell injection for BT48 and BT67 respectively. The first 2 doses were administered for 2 consecutive weeks as loading doses, followed by dosing every 2 weeks. Median survival of treated animals was significantly increased compared to vehicle-treated control animals in both models (Figure 6A). BT48: (vehicle vs 15 mg/kg BI-907828: 75 vs 102 days;  $P < .0001$ ; log-rank test; vehicle vs 50 mg/kg BI-907828: 75 vs 115 days, respectively;  $P < .0001$ ; log-rank test). BT67: (vehicle vs 15 mg/kg BI-907828: 163 vs 191 days;  $P < .0001$ ; log-rank test; vehicle vs 50 mg/kg BI-907828: 163 vs 189 days, respectively;  $P = .0002$ ; log-rank test). However, dose-dependent efficacy was only observed in the *MDM2* amplified BT48 model with the 50 mg/kg treatment, demonstrating a significant improvement in survival over the 15 mg/kg treatment arm (50 mg/kg BI-907828 vs 15 mg/kg BI-907828: 115 days vs 102 days;  $P < .001$ ) but not in the BT67 model.

Given that TMZ is a current standard of care for GBM, we further assessed whether a combinatorial treatment with TMZ (30 mg/kg weekly p.o.) would show efficacy over TMZ alone or the BI-907828 single-agent arm (15 mg/kg weekly p.o.). BT48 and BT67 both have *MGMT* promoter methylation and are sensitive to TMZ treatment in vitro (Supplemental Table 1, Figure 1). Interestingly, while improved survival was observed with long-term TMZ treatment in monotherapy in both models, a striking additional survival benefit was seen with a combinatorial treatment of 15 mg/kg BI-907828 + 30 mg/kg TMZ in the BT67 model (Figure 6). Given these results, we assessed whether combinatorial treatments with TMZ (30 mg/kg weekly p.o.) would improve efficacy over a single-agent treatment with TMZ alone or the BI-907828 single-agent arm (2 mg/kg or 15 mg/kg weekly p.o.) in another model, BT89, with a similar molecular profile as BT67 (Supplemental Table 1). Survival benefit was again observed in all the single treatment arms including the 2 mg/kg and 15 mg/kg BI-907828 dose groups (vehicle vs 2 mg/kg BI-907828: 163 vs 181 days;  $P < .006$ ; log-rank test; vehicle vs 15 mg/kg BI-907828: 163 vs 233 days, respectively;  $P < .0001$ ; log-rank test). Interestingly, similarly to BT67, an additional survival benefit was observed with a combinatorial treatment of 15 mg/kg BI-907828 + 30 mg/kg TMZ in the BT89 model (Figure 6). Survival was long-term and median survival was not reached for the animals from the 15 mg/kg BI-907828 + 30 mg/kg TMZ combinatorial treatment arm in either the BT67 or the BT89 model. All remaining animals were sacrificed at ~365 days post tumor cell injection at the study endpoint, at which point the remaining animals started displaying age-related co-morbidities and were sacrificed according to animal care guidelines.

### Treatment With BI-907828 Decreases Tumor Burden in Intracranial Orthotopic Xenograft Models

We further assessed the differences in tumor burden at the study endpoint in mice treated with BI-907828 compared to vehicle control mice. H&E staining and immunohistochemistry with an antibody specific for the human homolog of nucleolin demonstrated reduced tumor burden at endpoint in both BT48 and BT67 models in all arms of the study compared to vehicle controls (Supplemental Figure 5). These differences were especially noticeable in the *MDM2* amplified BT48 model. Immunostaining with the proliferation marker Ki67 further showed very few positive cells in either the 15 mg/kg or 50 mg/kg treated arms of the BT48 model and Ki67 in the 50 mg/kg treatment arm of the BT67 model. These results highlight that BI-907828 is highly effective at reducing tumor burden in BTSC-derived, orthotopic models of GBM.

## Discussion

GBM is a devastating disease with limited treatment options. Here, we show that BI-907828 is effective at reducing the viability of TP53 wild-type BTSCs irrespective of *MDM2* amplification status in vitro. BI-907828 further

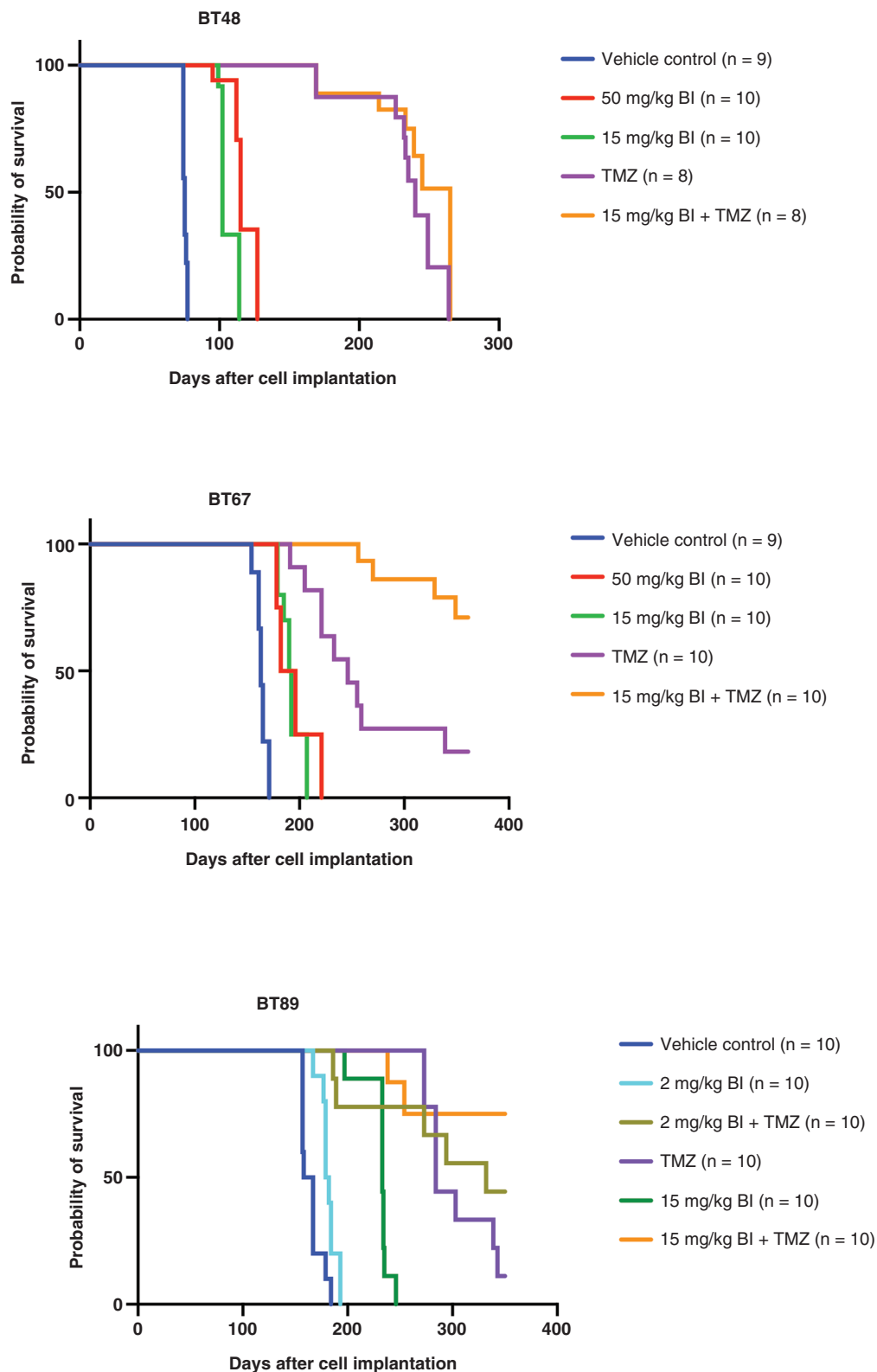


**Figure 6.** Long-term systemic administration of BI-907828 prolongs animal survival of mice orthotopically xenografted with *TP53* wild-type brain tumor stem cells (BTSCs). Oral administration of BI-907828 significantly increased median survival compared to vehicle treatments. Efficacy of temozolomide (TMZ) at a weekly oral dose of 30 mg/kg was observed in all three models. Additional benefit was seen in animals xenografted with BT67 and in BT89 with a combinatorial treatment of 15 mg/kg BI-907828 + TMZ.



demonstrates preclinical efficacy, penetrates the blood brain barrier (BBB), and significantly improves survival in three BTSC orthotopic xenograft models.

Our in vitro dose-response experiments with 11 TP53 wild-type BTSC lines demonstrate that BI-907828 reduces BTSC viability and induces cell death with IC50s at picomolar concentrations. BI-907828 has no obvious effect at similar concentrations in 8 TP53 mutant BTSC lines. We further confirmed that BI-907828 displays on-target activity and induces downstream p53 target genes that are effectors of cell cycle arrest (p21), and apoptosis (PUMA and cleaved PARP). These data further highlight that patients with TP53 wild-type mutational status would benefit from therapy with BI-907828 in a clinical setting.

In the past few years, several molecules have been developed to release p53 from the control of MDM2 and restore its tumor suppressor activity (reviewed in Ref. 23). Clinical data suggest thrombocytopenia is an on-target, dose-limiting toxicity for this class of inhibitors.<sup>17,23,25,26</sup> Thrombocytopenia could limit the clinical utility of MDM2 inhibitors in solid tumor indications. Hence there is a need for less frequently dosed MDM2 inhibitors to allow bone marrow recovery, mitigate clinical side effects and potentially improve the therapeutic window for these inhibitors. We show here that BI-907828 is a highly potent MDM2 inhibitor capable of achieving efficacy in preclinical mouse models of human GBM with less frequent dosing. Significant and striking differences in survival were achieved with a single weekly 15 mg/kg or bi-weekly dosing of 50 mg/kg BI-907828. In a follow-up study, we have further found that treatment with BI-902878 can be reduced to weekly doses as low as 2 mg/kg and 10 mg/kg and achieve efficacy in the MDM2 amplified BT48 and normal CN BT67 model, respectively (Supplemental Figure 5C). Thus, compared to currently available MDM2 inhibitors, the high potency, and the favorable pharmacokinetic properties of BI-907828 allow for optimized dose schedules that may reduce myelosuppression, an on-target, dose-limiting toxicity for this class of inhibitors, thereby presumably enabling the successful treatment of GBM tumors in humans.

A major challenge in investigating new treatment strategies for GBM is finding drugs that effectively penetrate the BBB. The previously described PK properties of BI-907828 enable a variety of different clinical dosing schedules with the potential to improve the therapeutic index with respect to on-target safety.<sup>27</sup> Our in vivo studies in three different orthotopic xenograft models of GBM clearly demonstrate that BI-907828 could be delivered to mice over a long period of time (>6 months) at low doses (2 mg/kg, 10mg/kg, and 15 mg/kg) once a week or higher doses (50 mg/kg) every 2 weeks with significant survival improvement. It was also evident that co-administration of BI-907828 and the standard of care, TMZ, was well tolerated in these models. In the context of combinatorial TMZ treatment with 15 mg/kg BI-907828, there was a striking survival improvement in the combinatorial arm in the BT67 and BT89 models. Our results provide a strong rationale for clinical testing of BI-907828, with the right dosing schedules to mitigate risks of myelosuppression and thrombocytopenia, in GBM patients with TP53 wild-type tumors, both as a single agent and in combination with the standard of care TMZ.

## Supplementary Material

Supplementary material is available online at *Neuro-Oncology* (<http://neuro-oncology.oxfordjournals.org/>).

## Keywords

brain tumor stem cells | glioblastoma | MDM2 | p53 | pre-clinical efficacy

## Funding

This research project was supported in part by Boehringer Ingelheim and by a grant from the Canadian Institutes of Health Research Reg. # 80550 6730 RR0001 (to H.A.L.).

## Acknowledgments

The authors thank Rozina Hassam for technical support and Dr Yaoqing Shen for genomic information analysis.

## Conflict of Interest

None.

## Authorship

**Conceptualization:** H.A.L., S.B., D.R.; **Methodology:** X.H., R.K.B., O.C., D.A.B., J.R., S.B., U.W.-C., H.A.L.; **Investigation:** X.H., R.K.B., O.C., D.A.B., J.R.; **Formal Analysis and Visualization:** H.A.L., X.H., R.K.B., S.B., and D.R.; **Writing:** H.A.L.; **Writing—Review and Editing:** D.R. and H.A.L. **Funding Acquisition:** H.A.L.; **Supervision:** H.A.L.

## References

1. Lane DP. Cancer. p53, guardian of the genome. *Nature*. 1992;358(6381):15–16.
2. Donehower LA, Harvey M, Slagle BL, et al. Mice deficient for p53 are developmentally normal but susceptible to spontaneous tumours. *Nature*. 1992;356(6366):215–221.
3. Olivier M, Hollstein M, Hainaut P. TP53 mutations in human cancers: origins, consequences, and clinical use. *Cold Spring Harbor Perspect Biol*. 2010;2(1):a001008.
4. Levine AJ, Oren M. The first 30 years of p53: growing ever more complex. *Nat Rev Cancer*. 2009;9(10):749–758.
5. Brooks CL, Gu W. p53 ubiquitination: Mdm2 and beyond. *Mol Cell*. 2006;21(3):307–315.

6. Kandath C, McLellan MD, Vandin F, et al. Mutational landscape and significance across 12 major cancer types. *Nature*. 2013;502(7471):333–339.
7. Lawrence MS, Stojanov P, Mermel CH, et al. Discovery and saturation analysis of cancer genes across 21 tumour types. *Nature*. 2014;505(7484):495–501.
8. Stupp R, Mason WP, van den Bent MJ, et al. Radiotherapy plus concomitant and adjuvant temozolomide for glioblastoma. *N Engl J Med*. 2005;352(10):987–996.
9. Ohgaki H, Kleihues P. Genetic pathways to primary and secondary glioblastoma. *Am J Pathol*. 2007;170(5):1445–1453.
10. Cancer Genome Atlas Research Network. Comprehensive genomic characterization defines human glioblastoma genes and core pathways. *Nature*. 2008;455(7216):1061–1068.
11. Verhaak RGW, Hoadley KA, Purdom E, et al; Cancer Genome Atlas Research Network. Integrated genomic analysis identifies clinically relevant subtypes of glioblastoma characterized by abnormalities in PDGFRA, IDH1, EGFR, and NF1. *Cancer Cell*. 2010;17(1):98–110.
12. Konopleva M, Martinelli G, Daver N, et al. MDM2 inhibition: an important step forward in cancer therapy. *Leukemia*. 2020;34(11):2858–2874.
13. Haupt Y, Maya R, Kazaz A, Oren M. Mdm2 promotes the rapid degradation of p53. *Nature*. 1997;387(6630):296–299.
14. Ventura A, Kirsch DG, McLaughlin ME, et al. Restoration of p53 function leads to tumour regression in vivo. *Nature*. 2007;445(7128):661–665.
15. Xue W, Zender L, Miething C, et al. Senescence and tumour clearance is triggered by p53 restoration in murine liver carcinomas. *Nature*. 2007;445(7128):656–660.
16. Martins CP, Brown-Swigart L, Evan GI. Modeling the therapeutic efficacy of p53 restoration in tumors. *Cell*. 2006;127(7):1323–1334.
17. Zhao Y, Bernard D, Wang S. Small molecule inhibitors of MDM2-p53 and MDMX-p53 interactions as new cancer therapeutics. *BioDiscovery*. 2013;4(8):4.
18. Ding Q, Zhang Z, Liu J-J, et al. Discovery of RG7388, a potent and selective p53-MDM2 inhibitor in clinical development. *J Med Chem*. 2013;56(14):5979–5983.
19. Jeay S, Ferretti S, Holzer P, et al. Dose and schedule determine distinct molecular mechanisms underlying the efficacy of the p53-MDM2 inhibitor HDM201. *Cancer Res*. 2018;78(21):6257–6267.
20. Jiang L, Zawacka-Pankau J. The p53/MDM2/MDMX-targeted therapies—a clinical synopsis. *Cell Death Dis*. 2020;11(4):237.
21. Reis B, Jukofsky L, Chen G, et al. Acute myeloid leukemia patients clinical response to idasanutlin (RG7388) is associated with pretreatment MDM2 protein expression in leukemic blasts. *Haematologica*. 2016;101(5):e185–e188.
22. Rew Y, Sun D. Discovery of a small molecule MDM2 inhibitor (AMG 232) for treating cancer. *J Med Chem*. 2014;57(15):6332–6341.
23. Tisato V, Voltan R, Gonelli A, Secchiero P, Zauli G. MDM2/X inhibitors under clinical evaluation: perspectives for the management of hematological malignancies and pediatric cancer. *J Hematol Oncol*. 2017;10(1):133.
24. Skalniak L, Kocik J, Polak J, et al. Prolonged idasanutlin (RG7388) treatment leads to the generation of p53-Mutated cells. *Cancers (Basel)*. 2018;10(11):396.
25. Hyman D, Chatterjee M, Langenberg MHG, et al. Dose- and regimen-finding phase I study of NVP-HDM201 in patients (pts) with TP53 wild-type (wt) advanced tumors. *Eur J Cancer*. 2016;69:S128–S129.
26. Gounder MM, Bauer TM, Schwartz GK, et al. Milademetan, an oral MDM2 inhibitor, in well-differentiated/ dedifferentiated liposarcoma: results from a phase 1 study in patients with solid tumors or lymphomas. *Eur J Cancer*. 2020;138:S3–S4.
27. Rinnenthal J, Rudolph D, Blake S, et al. Abstract 4865: BI 907828: A highly potent MDM2 inhibitor with low human dose estimation, designed for high-dose intermittent schedules in the clinic. *Exp Mol Ther*. 2018;78(suppl 13):4865.
28. Rudolph D, Gollner A, Blake S, et al. Abstract 4868: BI 907828: a novel, potent MDM2 inhibitor that is suitable for high-dose intermittent schedules. *Exp Mol Ther*. 2018;78(suppl 13):4868.
29. Rudolph D, Reschke M, Blake S, et al. Abstract 4866: BI 907828: a novel, potent MDM2 inhibitor that induces antitumor immunologic memory and acts synergistically with an anti-PD-1 antibody in syngeneic mouse models of cancer. *Exp Mol Ther*. 2018;79(suppl 13):3197.
30. Rudolph D, Weyer-Czernilofsky U, Reschke M, et al. Abstract 3197: BI-907828, a novel and potent MDM2-p53 antagonist, acts synergistically in a triple combination with anti-PD-1 and anti-LAG-3 antibodies in syngeneic mouse models of cancer. *Immunology*. 2019;79(suppl 13):3197.
31. Luchman HA, Bozek D, Hao X, et al. Abstract 3084: BI-907828: a novel, potent MDM2 inhibitor, inhibits GBM brain tumor stem cells in vitro and prolonged survival in orthotopic xenograft mouse models. *Exp Mol Ther*. 2019. doi: [10.1158/1538-7445.sabcs18-3084](https://doi.org/10.1158/1538-7445.sabcs18-3084).
32. Cornillie J, Wozniak A, Li H, et al. Anti-tumor activity of the MDM2-TP53 inhibitor BI-907828 in dedifferentiated liposarcoma patient-derived xenograft models harboring MDM2 amplification. *Clin Transl Oncol*. 2020;22(4):546–554.
33. Boehringer Ingelheim. <https://www.inoncology.com/ourpipeline/mdm2-p53-antagonist>. Accessed January 9, 2021.
34. Website. ClinicalTrials.gov. NCT03449381. <https://clinicaltrials.gov/ct2/show/NCT03449381>; <https://clinicaltrials.gov/ct2/show/NCT05218499>; <https://clinicaltrials.gov/ct2/show/NCT05512377>; <https://clinicaltrials.gov/ct2/show/NCT05218499>. Accessed November 16, 2022.
35. Jensen KV, Cseh O, Aman A, Weiss S, Luchman HA. The JAK2/STAT3 inhibitor pacritinib effectively inhibits patient-derived GBM brain tumor initiating cells in vitro and when used in combination with temozolomide increases survival in an orthotopic xenograft model. *PLoS One*. 2017;12(12):e0189670.
36. Kelly JJP, Stechishin O, Chojnacki A, et al. Proliferation of human glioblastoma stem cells occurs independently of exogenous mitogens. *Stem Cells*. 2009;27(8):1722–1733.
37. Luchman HA, Stechishin OD, Dang NH, et al. An in vivo patient-derived model of endogenous IDH1-mutant glioma. *Neuro Oncol*. 2012;14(2):184–191.
38. Luchman HA, Stechishin ODM, Nguyen SA, et al. Dual mTORC1/2 blockade inhibits glioblastoma brain tumor initiating cells in vitro and in vivo and synergizes with temozolomide to increase orthotopic xenograft survival. *Clin Cancer Res*. 2014;20(22):5756–5767.
39. Cusulin C, Chesnelong C, Bose P, et al. Precursor states of brain tumor initiating cell lines are predictive of survival in xenografts and associated with glioblastoma subtypes. *Stem Cell Rep*. 2015;5(1):1–9.
40. Jones SJ, Laskin J, Li YY, et al. Evolution of an adenocarcinoma in response to selection by targeted kinase inhibitors. *Genome Biol*. 2010;11(8):R82.
41. Macleod G. al. Genome-wide CRISPR-Cas9 screens expose genetic vulnerabilities and mechanisms of temozolomide sensitivity in glioblastoma stem cells. *Cell Rep*. 2019;27:971–986.
42. Shen Y, Grisdale CJ, Islam SA, et al. Comprehensive genomic profiling of glioblastoma tumors, BTICs, and xenografts reveals stability and adaptation to growth environments. *Proc Natl Acad Sci USA*. 2019;116(38):19098–19108.
43. Ostermann S, Csajka C, Buclin T, et al. Plasma and cerebrospinal fluid population pharmacokinetics of temozolomide in malignant glioma patients. *Clin Cancer Res*. 2004;10(11):3728–3736.